JACS
JOURNAL OF THE AMERICAN CHEMICAL SOCIETY

Article

pubs.acs.org/JACS

Intracellular Delivery of Functional Proteins and Native Drugs by Cell-Penetrating Poly(disulfide)s

Jiaqi Fu,[†] Changmin Yu,[†] Lin Li,[†,‡] and Shao Q. Yao*[,†]

[†]Department of Chemistry, National University of Singapore, 117543 Singapore

[‡]Key Laboratory of Flexible Electronics and Institute of Advanced Materials, National Jiangsu Synergistic Innovation Center for Advanced Materials, Nanjing Tech University, Nanjing 211816, P. R. China

Supporting Information

ABSTRACT: The efficient delivery of bioactive compounds into cells is a major challenge in drug discovery. We report herein the development of novel methods for intracellular delivery of functional proteins (including antibodies) and native small-molecule drugs by making use of cell-penetrating poly(disulfide)s (CPDs). CPDs were recently shown to be rapidly taken up by mammalian cells in endocytosis-independent pathways, but their applications for delivery of proteins and native small-molecule drugs have not been demonstrated. With our newly developed, CPD-assisted approaches, rapid and "bioorthogonal" loading of cargos was carried out with pre-synthesized CPDs, in two steps and in a matter of minutes under aqueous conditions. The resulting CPD−cargo conjugates were used immediately for subsequent cell delivery studies. With the versatility and flexibility of these methods, we further showed that they could be used for immediate delivery of a variety of functional cargos with minimum chemical and genetic manipulations. The minimal cell cytotoxicity of these CPDs and their cargo-loaded conjugates further highlights the unique advantage of this new cell-transduction method over other existing strategies and ensures that our entire delivery protocol is compatible with subsequent live-cell experiments and biological studies.

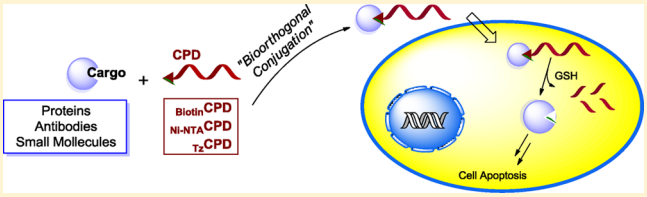

INTRODUCTION

The efficient delivery of bioactive compounds, including nucleic acids, peptides/proteins, and small molecules, into cells is a major challenge in drug discovery.[1] The difficulty is more pronounced for large molecules such as proteins and DNAs/RNAs,[2] but because of their hydrophobicity and poor water solubility, many small-molecule drug candidates also do not enter cells readily without proper formulation and/or delivery vehicles.[3] To achieve intracellular delivery of proteins, a variety of methods have been developed in the past 20 years, including those using cell-penetrating peptides (CPPs), supercharged proteins, liposomes, nanoparticles (NPs), and polymers.[4−7] Despite significant progress, these methods have their share of shortcomings, including low/variable delivery efficiency, the need for protein modification, high cytotoxicity, and, perhaps most importantly, ineffective endosomal/lysosomal escape.[2a] Taking CPPs for example, it is well-documented that, while CPP-conjugated small- and medium-size cargos may be efficiently transduced into cells via non-endocytic pathways, large cargos such as proteins are mostly taken up by endocytosis, leading to subsequent endosomal trapping and lysosomal degradation.[8] To deliver hydrophobic small molecules intracellularly, chemical modifications may be used to make analogues that possess improved physicochemical and pharmacokinetic profiles,[9] but this is costly and time-consuming, and worse, it often results in alteration of the compound's biological properties.[3b] Recent advances in materials chemistry have provided alternatives, where native drugs are directly "loaded" into a suitable "container" without the need of chemical modifications.[3a,10] For example, the use of small-molecule-encapsulated mesoporous silica nanoparticles (MSNs) for drug delivery is worth noting, in part due to the numerous desirable properties that MSNs possess, including high loading capacity, biocompatibility, and "zero premature release".[10b,c] In order to minimize unwanted leakage of the encapsulated drug and improve cellular uptake of MSNs, the surfaces of these NPs are "capped" with CPPs and other forms of chemicals,[11] which, in most cases, also leads to severe endosome trapping and ineffective drug release.[11a,b]

Herein, we focus on the development of novel methods for intracellular delivery of functional proteins (including antibodies, Abs) and native small-molecule drugs by making use of cell-penetrating poly(disulfide)s (CPDs) (Figure 1A).[12] CPDs could be considered synthetic mimics of poly-arginine CPPs, in which the polypeptide backbone was replaced with poly(disulfide)s. Upon cellular uptake, CPDs are rapidly degraded in the cytosol by glutathione (GSH)-assisted depolymerization and show minimal cytotoxicity.[12,13] Importantly, Matile et al. showed in a recent study that CPDs made of thiol-modified small fluorophores (as initiators/cargos), a guanidinium-propagating monomer (e.g., **M** in Figure 1A), and a terminator (e.g., **T**) rapidly enter mammalian cells via thiol-mediated pathways.[12b] The major issue of endosomal trapping commonly

Received: August 7, 2015
Published: September 4, 2015

DOI: 10.1021/jacs.5b08130
J. Am. Chem. Soc. 2015, 137, 12153−12160

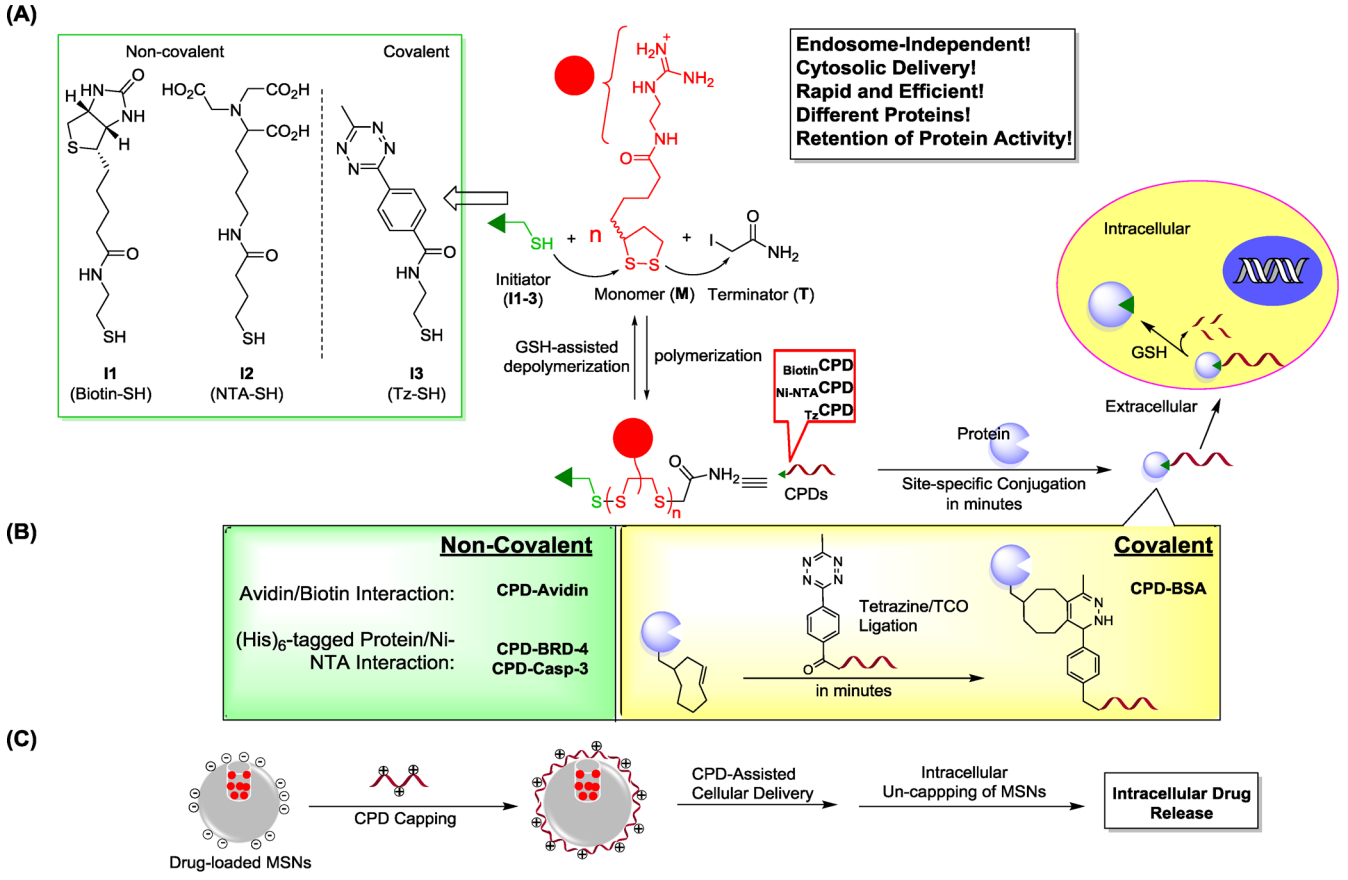

		CPD				
		Mw (KDa)	PDI	Cargo	Complexed Product	Formation via
Protein	$_{Biotin}$CPD	30	1.5	Avidin^{Cy5}	CPD-Avidin	Non-Covalent Affinity Interaction
	$_{Ni\text{-}NTA}$CPD	32	1.6	BRD-4^{Cy5}	CPD-BRD-4	
				Casp-3	CPD-Casp-3	
	$_{Tz}$CPD	22	2.3	TCO-BSA^{Cy5}	CPD-BSA	Covalent Bioorthogonal Ligation
				TCO-Ab^{FC}	CPD-Ab	
Small Molecule	$_{Biotin}$CPD	30	1.5	MSN-Dox	CPD-MSN-Dox	Charge Interaction

Figure 1. Overview of CPD-facilitated intracellular delivery of proteins (including antibodies) and native small-molecule drugs. (A) Newly developed initiators (**I1**/**I2**/**I3**), monomer (**M**), terminator (**T**), the polymerization/depolymerization process of CPDs, and the two-step approach for "conjugation" of protein cargos with CPDs. (B) Summary of non-covalent and covalent approaches for bioorthogonal attachment of CPDs to proteins. The highly efficient site-specific tetrazine–*trans*-cyclooctyne (TCO) ligation reaction is highlighted. (C) Schematic summary of intracellular delivery of native small molecules by drug-loaded MSNs capped with $_{Biotin}$**CPD**. (D) Summary of all CPDs and cargos used in the current study.

associated with CPPs and other means of delivery was thus minimized.[14] Subsequently, the authors proposed that these substrate-initiated cell-penetrating poly(disulfide)s (siCPDs) may be used for intracellular delivery of other thiol-containing (or modified) cargos. This hypothesis, however, was never demonstrated experimentally. Furthermore, during siCPD synthesis, given the obligatory role of the thiol-containing initiator (**I**) and the need for millimolar concentrations of initiator/monomer/terminator as well as organic co-solvents, it is not trivial how a protein could be directly used as an initiator, nor is it practical to use thiol-modified small-molecule drugs, as few small-molecule drugs contain native thiols in their structures.

With the current work, we have confirmed that, for the first time, proteins conjugated with CPDs, either covalently (via bioorthogonal chemistry) or non-covalently (via affinity interaction), could be rapidly and efficiently delivered into the cytosol of different mammalian cells without being trapped by endocytic vesicles. Similarly, by making use of CPD-capped MSNs, we have successfully achieved intracellular delivery of native small-molecule drugs (e.g., doxorubicin, Dox). Our results indicate that these novel protein and small-molecule delivery methods possess the following favorable properties when compared to most existing strategies: (1) fast delivery, with cell entry in less than 15 min; (2) flexible, enabling convenient delivery of different types of cargos; (3) less cytotoxic, and applicable to different types of mammalian cells;

DOI: 10.1021/jacs.5b08130
J. Am. Chem. Soc. 2015, 137, 12153−12160

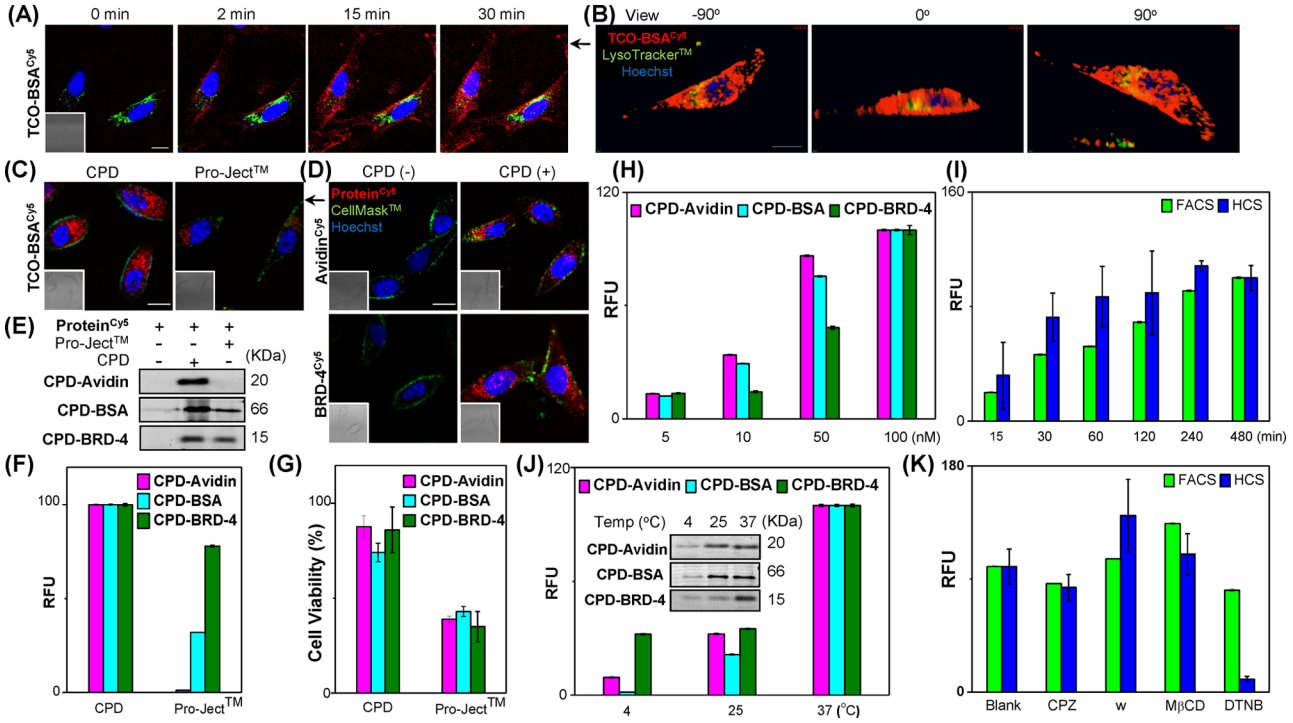

Figure 2. Cellular uptake of CPD-conjugated proteins. (A) Real-time CLSM of live HeLa cells treated with 50 nM of **CPD-BSA** (red), LysoTracker (green), and Hoechst (blue) at indicated time intervals. Inset: bright-field image of the corresponding fluorescence channels. Scale bar = 20 μm. (B) 3D projections of *z*-stack images at different perspectives (step size, 0.186 μm) of HeLa cells 2 h after **CPD-BSA** delivery. Pearson coefficient R = 0.35 (red/green). Scale bar = 13.2 μm. See supplementary videos S1–S5 for details. (C) CLSM images showing cellular uptake of **CPD-BSA** (50 nM) versus **TCO-BSA**^{Cy5} (50 nM) complexed to Pro-Ject reagent. The images were taken 1 h after protein delivery. Cells with the delivered proteins (red) were co-stained with CellMask membrane tracker (green) and Hoechst (blue). Inset: bright-field images. Scale bar = 20 μm. (D) Same as (C), except **CPD-Avidin** (top) or **CPD-BRD-4** (bottom) was used, with the corresponding CPD-free **Avidn**^{Cy5} or **BRD-4**^{Cy5} serving as negative control. (E) SDS-PAGE/in-gel fluorescence scanning of lysates from HeLa cells treated with **CPD-Protein** (50 nM each; 1 h incubation), showing successful cellular uptake. Cells treated with the corresponding CPD-free protein (50 nM; 1 h incubation), either with or with Pro-Ject reagents, were run concurrently as controls. (F) Quantitative analysis of CPD-assisted protein delivery to HeLa cells by flow cytometry. Control experiments were done with the Pro-Ject method on the same proteins. Surface-bound fluorescent materials were removed by washing the cells with heparin-containing PBS. RFU = relative fluorescence units. Data from the Pro-Ject results were normalized to each of the CPD-delivered experiments. (G) Cell viability measured with XTT assay for HeLa cells treated with a protein (50 nM; 1 h incubation) delivered by either CPD or Pro-Ject method. Buffer-treated cells were used for normalization (as 100% viability). (H) Concentration-dependent protein delivery to HeLa cells as determined by flow cytometry analysis (FACS). Cells were treated with each protein (5, 10, 50, 100 nM) for 8 h before being quantified. The overall uptake for each protein at different concentrations was normalized to data obtained at 100 nM. (I) Time-dependent protein uptake of HeLa cells treated with **CPD-BSA** (50 nM). The protein uptake was quantified by both flow cytometry and high-content screening (HCS) of live cells. The overall uptake in each experiment was normalized to the data obtained at 8 h. (J) Temperature-dependent protein uptake by HeLa cells (50 nM protein; 1 h treatment), as determined by flow cytometry. Data were normalized to those obtained at 37 °C. Inset: SDS-PAGE/in-gel fluorescence scanning of lysates from treated cells. (K) Flow cytometry/HCS quantification of protein uptake (50 nM of **CPD-BSA**; 1 h incubation) by HeLa cells treated with different inhibitors, including chlorpromazine (CPZ), wortmannin (w), methyl-β-cyclodextrin (MβCD), and 5,5′-dithiobis-2-nitrobenzoic acid (DTNB). Data were normalized to those of HeLa cells treated with **CPD-BSA** only (Blank).

(4) efficient, facilitating cargo delivery at nanomolar concentrations; and (5) immediately available upon cell entry due to rapid CPD degradation, thus retaining the biological activity of the delivered cargo.

RESULTS AND DISCUSSION

Design and Synthesis of New CPDs. We were intrigued by the excellent properties of siCPDs (e.g., minimal endosome trapping and cytotoxicity), as reported by Matile et al.,[12] and wondered whether robust, CPD-mediated methods could be developed to facilitate intracellular delivery of functional proteins, therapeutic antibodies, and native small-molecule drugs (that is, without any form of thiol modification). Instead of the siCPD synthesis as originally proposed,[12b] we envisaged such cargos could be more conveniently appended, in two steps, to pre-synthesized, functionally decorated CPDs by using suitable "conjugation" chemistries that are already available for recombinant proteins/antibodies and small molecules (Figure 1). Three types of thiol-containing initiators, **I1**, **I2**, and **I3**, were thus designed, containing biotin, nitrilotriacetic acid (NTA), and tetrazine (Tz), respectively. Upon polymerization, the corresponding CPDs ($_{Biotin}$**CPD**, $_{Ni\text{-}NTA}$**CPD**, and $_{Tz}$**CPD**; Figure 1D) could be obtained. $_{Ni\text{-}NTA}$**CPD** could be attached bioorthogonally to readily available $(His)_6$-tagged proteins via non-covalent affinity interaction (K_d of Ni-NTA/$(His)_6$ $<10^{-7}$ M). $_{Biotin}$**CPD** was designed to test whether it could be used to deliver avidin via similar non-covalent, but substantially stronger, interactions (K_d of biotin/avidin $<10^{-15}$ M). For a therapeutic Ab, which might not possess a his-tag,[15] we used the well-known bis-sulfone chemistry that enables site-specific introduction of a *trans*-cyclooctyne (TCO) into the native disulfide present in the Ab (*vide infra*).[16] Subsequent bioorthogonal covalent attachment of $_{Tz}$**CPD** to the TCO-

DOI: 10.1021/jacs.5b08130
J. Am. Chem. Soc. 2015, 137, 12153–12160

modified Ab would result in quantitative formation of **CPD-Ab** within minutes by the highly efficient Tz−TCO ligation (Figure 1B).[17] To "append" a native small-molecule drug to the CPD, we would use a positively charged CPD ($_{Biotin}$**CPD** in this case) to cap the negatively charged, drug-loaded MSNs (i.e., **MSN-Dox**) by electrostatic interaction, giving **CPD-MSN-Dox** (Figure 1C,D); the capping of NPs with CPDs is unprecedented, and we were hopeful that, if CPDs could facilitate endocytosis-independent cellular uptake of large, nanometer-size cargos such as MSNs, then a variety of hydrophobic drugs could potentially be delivered intracellularly in their native form, in a controllable manner.[10]

All three initiators were conveniently synthesized (two in their respective disulfide forms; Scheme S1) and treated/reduced with TECP immediately prior to polymerization. The monomer (**M**) and subsequent polymerized products with the corresponding initiators (and capped with **T**; Figure 1A) were synthesized according to published protocols.[12b] Upon purification, the resulting CPDs were further characterized by gel permeation chromatography, giving an average molecular weight of 22−32 kDa with a polydispersity index of 1.5−2.3 (Figures 1D and S3A). The concentration of $_{Tz}$**CPD** stock solution was determined by measurement with UV−vis spectroscopy at the Tz absorbance ($\lambda_{520\ nm}$);[18] the concentrations were similarly estimated for the other two CPDs.

Protein Attachment to CPDs. We next chose three fluorescently labeled recombinant proteins having different molecular weights, **Avidin**^{Cy5} (∼80 kDa in its tetrameric form), **TCO-BSA**^{Cy5} (∼66 kDa), and **BRD-4**^{Cy5} (∼15 kDa; an epigenetic reader protein[19]) as model cargos for delivery by $_{Biotin}$**CPD**, $_{Tz}$**CPD**, and $_{Ni\text{-}NTA}$**CPD**, respectively. Fluorescent labeling of these proteins was done by standard protein conjugation chemistry with commercially available Cy5 dyes (Figure S1), thus allowing the entire cargo delivery process to be monitored by fluorescence microscopy and quantified by flow cytometry. Attachment of CPDs, either non-covalently or covalently, to the proteins was next done by simple "mix-and-go" protocols, giving **CPD-Avidin**, **CPD-BSA**, and **CPD-BRD-4**, respectively (Figures 1D and S2). It should be highlighted that our choices of highly bioorthogonal "conjugation" chemistries between CPDs and proteins were critical, not only for the sake of convenience and generality but, more importantly, also to allow protein complexes to be directly used in subsequent cell-based experiments. Furthermore, since most CPD/protein-complexing reactions could not be reliably monitored by sodium dodecyl sulfide−polyacrylamide gel electrophoresis (SDS-PAGE) without addition of dithiothreitol (DTT), which in turn caused CPD degradation (data not shown), we needed such conjugation chemistries to be free of failure! Nevertheless, we found that **Avidin**^{Cy5} and **CPD-Avidin** were well separated under modified DTT-free SDS-PAGE conditions (presumably due to extremely strong biotin/avidin interaction and avidin stability[20]), and they were thus chosen as the model system to monitor the processes of CPD/protein complex formation and GSH-assisted intracellular depolymerization/cargo release (Figure S3B); upon incubation with a freshly prepared HeLa lysate (1 mg/mL) for 1 h at 37 °C, the higher-order **CPD-Avidin** complex was found to have significantly depolymerized, indicating that our CPD-loaded protein cargos would also be released readily in cytosolic environments.

Cellular Uptake. In order to unequivocally demonstrate the cellular uptake of the CPD-conjugated proteins and their subcellular localization, we used confocal laser scanning microscopy (CLSM) with live HeLa cells. It was previously found that the use of fixed cells are not suitable for such studies;[8b] upon fixation, cargos delivered by CPPs and other means often artificially "escape" from endocytic vesicles, thus resulting in misleading conclusions.[2a,21] Real-time imaging experiments together with different fluorescent organelle trackers (CellMask membrane tracker/LysoTracker, pseudocolored in green; Hoechst nuclear stain, pseudocolored in blue) were carried out. As shown in Figure 2A, 2 min after addition of 50 nM of **CPD-BSA** (pseudocolored in red) to the culture medium at 37 °C, red fluorescence started to accumulate around the cell membrane. After 15 min, a substantial amount of **CPD-BSA** was observed to have successfully been transduced and evenly distributed throughout the cytosolic space, with no evidence of endosome/lysosome trapping. This trend persisted for the next 2 h (Figures 2B and S4, and supplementary videos S1−S5). With prolonged incubation (>4 h), however, we started to observe some merged green/red fluorescence signals, indicating that some delivered protein had been destined for lysosomal degradation, presumably due to high protein concentration or unfolding.[2a] We next directly compared the cellular uptake efficiency of this **CPD**-assisted strategy with that of the Pro-Ject reagent, a commercially available liposome-based protein delivery system.[22] In addition to CLSM (Figure 2C,D), we analyzed the successfully delivered and depolymerized proteins by SDS-PAGE/in-gel fluorescence scanning of lysates from treated cells (Figure 2E). We further quantified protein uptake by flow cytometry analysis (Figure 2F). In order to minimize false readings of cells derived from membrane-bound, but not internalized, fluorescent proteins, cells were washed with heparin-containing phosphate-buffered saline (PBS) before analysis.[12b] In all cases, with all three protein cargos (**TCO-BSA**^{Cy5}, **Avidin**^{Cy5}, and and **BRD-4**^{Cy5}) having different types of "conjugation" chemistries (covalent and non-covalent), their resulting CPD complexes (**CPD-BSA**, **CPD-Avidin**, and **CPD-BRD-4**) were delivered into HeLa cells more efficiently than the Pro-Ject delivery method. Successful intracellular uptake of a cargo was found to be completely dependent on its complex formation with the corresponding CPD, as none of the cargos alone (Figure 2D, left panels, and E, lane 1) could enter cells. We found that, unlike the liposome-based Pro-Ject method which makes use of electrostatic/hydrophobic interaction for complex formation with a target protein (thus delivery efficiency varies significantly with protein size/charge; see Figures 2E,F and S5),[22] proteins of different sizes and charges were efficiently delivered by the CPD-assisted method. Gratifyingly, even $(His)_6$-tagged proteins formed by comparatively moderate non-covalent interaction with $_{Ni\text{-}NTA}$**CPD** (e.g., **CPD-BRD-4**) could be delivered, thus setting the stage for more widespread applications of this new protein transduction technology in future. In addition, we found that the CPD method was significantly less cytotoxic than the Pro-Ject approach for protein delivery (Figure 2G). This is in good agreement with previous cell-based experiments with fluorophore-loaded siCPDs.[12b] In fact, the 10−20% cell death observed in our experiments was likely caused by trace amount of residual iodoacetamide from the polymerization reaction, which could not be completely removed with current purification method. Further optimizations of **CPD-Protein** delivery were done by concentration- and time-dependent experiments (Figures 2H,I and S6). In addition to flow cytometry, we used imaging-based, high-content screening

DOI: 10.1021/jacs.5b08130
J. Am. Chem. Soc. 2015, 137, 12153−12160

(HCS) for comparative studies. HCS could be used to simultaneously analyze many live cells in the same experiment, without cell detachment/fixation which might cause artifacts, thus was a quantitative complement to our CLSM results. As expected, both longer incubation time and higher cargo loading led to increases in the amount of delivered proteins. With the issues of potential lysosomal degradation and cytotoxicity in mind, we recommend the optimal conditions for this CPD delivery method to be 25−50 nM protein loading and 1−2 h incubation, which are still more efficient than existing protein delivery strategies.[4−7] The CPD method was further tested on other mammalian cell lines (NIH 3T3, MCF-7, A549, and PC3; Figure S7); in all cases, **CPD-BSA** was successfully taken up intracellularly, albeit at varying degrees of efficiency.

Our earlier CLSM results showed even cytosolic distribution of intracellular fluorescence upon protein delivery (Figure 2A−D), indicative of endocytosis-independent pathways facilitated by these CPDs, as previously proposed.[12b] In order to further confirm this, we carried our detailed uptake studies of **CPD-Protein** by HeLa cells at different temperatures and in the presence of endocytosis inhibitors (Figures 2J,K and S8); in general, cell uptake profiles observed with these CPD-conjugated proteins were similar to what was previously reported with small fluorophore-modified siCPDs.[12b] Reduced temperature decreased protein delivery efficiency but did not block the process completely (Figure 2J). The insensitivity of protein delivery to endocytosis-related inhibitors used (chlorpromazine, wortmannin, and methyl-β-cyclodextrin) ruled out the endocytosis pathway. On the contrary, blocking exofacial thiols on the cell surface with 5,5′-dithiobis-2-nitrobenzoic acid significantly suppressed protein uptake, further supporting thiol-mediated cargo delivery mechanisms.[12b] In our hands, flow cytometry gave less consistent results, presumably due to nonspecific, surface-bound **CPD-Protein** and the need of cell detachment (Figure 2K). HCS, on the other hand, was more reliable, enabling direct quantification of live cells having only intracellular fluorescence signals.

CPD-Assisted Transduction of Functionally Active Caspase-3. Having confirmed the effect of this newly developed CPD method for intracellular protein delivery with minimal endosome trapping, we next investigated whether it could deliver functional, therapeutic proteins. Caspase-3 (a cysteine protease) is a promising therapeutic protein owing to its key role in cell apoptosis.[23] Intracellular delivery of active caspase-3 to tumor cells renders them hypersensitive toward treatment by anticancer drugs such as Dox.[24] Functionally active, recombinant $(His)_6$-tagged caspase-3 was prepared as previously described.[25] Upon mixing with $_{Ni\text{-}NTA}$**CPD**, the resulting **CPD-Casp-3** was formed. Mindful of the trace amount of iodoacetamide from CPD preparation and that the absence of DTT might further reduce the enzymatic activity of caspase-3,[23] we carried out normalization of **CPD-Casp-3** (Figure S9); results indicate that even without DTT, **CPD-Casp-3** was able to retain >20% of the original caspase-3 activity. The activity of the complex was partially restored upon DTT treatment, presumably due to either CPD depolymerization or/and DTT reduction of active-site cysteine in the enzyme. Therefore, for **CPD-Casp-3**, upon cell entry, its enzymatic activity would also be restored under the highly reduced cytosolic environment. HeLa cells were incubated with 50 nM **CPD-Casp-3**, and the resulting cells were imaged for intracellular caspase-3 activity upon treatment with Ac-DEVD-AMC for 2 h (Figure 3A);[26] significant fluorescence signals

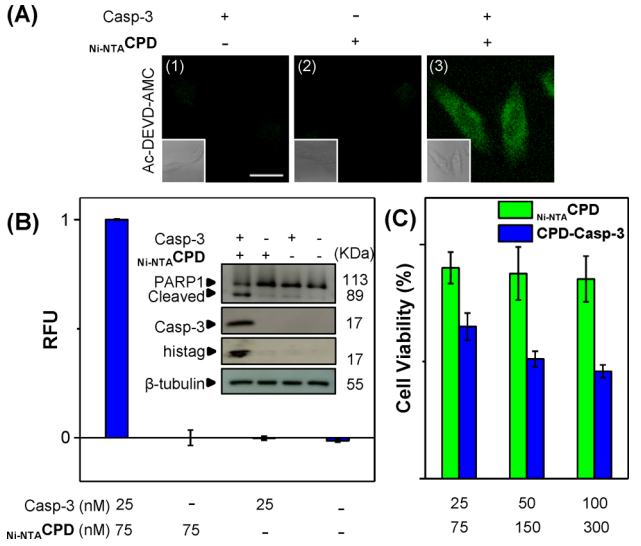

Figure 3. CPD-assisted delivery of functionally active caspase-3 to HeLa cells. (A) CLSM images of HeLa cells treated with **CPD-Casp-3** (50 nM) for 2 h, followed by incubation with Ac-DEVD-AMC (40 μM; 2 h). Scale bar = 20 μm. Inset: bright-field images. (B) RFU of *in vitro* enzymatic caspase-3 assay of treated HeLa lysates.[11c,27] Inset: WB results of delivered active caspase-3 and cleaved endogenous PARP1 in HeLa lysates from the same cells. (C) Cell viability/apoptosis caused by delivered active caspase-3 as measured by XTT assay. Since it took some time for intracellular caspase-3 to be translocated into the nucleus and cleave PARP1,[28] for panels (B) and (C), HeLa cells were treated with **CPD-Casp-3** for 8 h prior to analysis.

(from the liberated AMC dye) throughout the cytosol of **CPD-Casp-3**-treated cells, but not in control cells, were detected, indicating successful cytosolic delivery of the functionally active protein. These results were further confirmed by *in vitro* enzymatic determination of caspase-3 activity, as well as Western blotting (WB) analysis, of the corresponding cell lysates (Figure 3B);[11c,27] in all cases, the presence of intracellular caspase-3 and its activity were unequivocally established. Intracellular activation of caspase-3 is known to promote subsequent translocation of the active enzyme into nucleus, cleave PARP1, and finally cause cell death by apoptosis.[28] We observed similar phenomena in our "artificially" induced apoptotic cells as well (Figure 3B, inset, and C). These results further suggest that cytosolic proteins delivered by this CPD system are not necessarily confined to their original destination upon cell entry. Instead, they may be further sorted/translocated in manners similar to endogenous proteins.

CPD-Assisted Antibody Delivery. Monoclonal antibodies (mAbs) constitute one of the largest classes of therapeutic proteins.[29] There are currently more than 30 Ab-based, FDA-approved drugs, most of which target cancer. The number could have been much higher, had an effective means for intracellular delivery of Abs been available.[15] Common protein delivery methods are even more problematic for intracellular delivery of Abs, as most of them are large (>150 kDa). Realizing the highly efficient, endosome-independent features endowed by our newly developed CPD protein delivery method, we anticipated it might be ideally suited for delivery of therapeutic Abs, for which many robust conjugation chemistries are already available in the forms of antibody−drug conjugates (ADCs) and PEGylation, without compromising the Abs' activities and stabilities.[15,16a,30,31] We used Alexa

DOI: 10.1021/jacs.5b08130
J. Am. Chem. Soc. 2015, 137, 12153−12160

Fluor 488 goat anti-rabbit IgG (Ab^{FC}) as a model Ab and modified it with a commercially available bis-sulfone reagent, ThioLinker-TCO (Figure 4A);[16c] upon TCEP reduction of

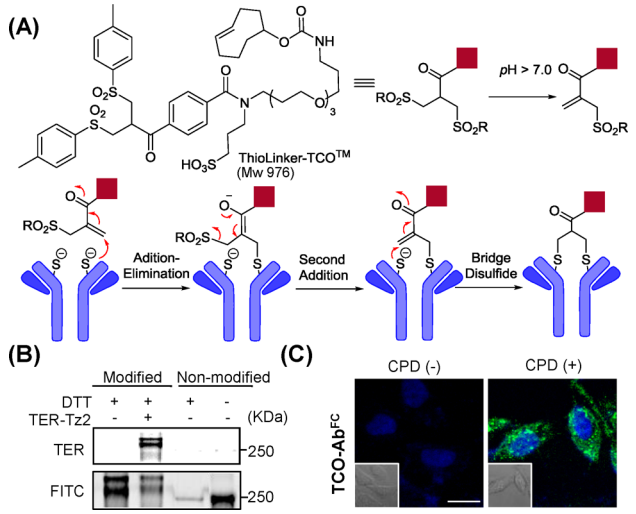

Figure 4. (A) Labeling mechanism of antibodies by ThioLinker-TCO. (B) **TCO-Ab^{FC}** reacting with or without TER-Tz2, before being analyzed by SDS-PAGE (with or without 10 mM DTT in the loading dye). The gel was visualized under both FITC and TER channels. (C) HeLa cells treated with 50 nM of **CPD-Ab** (1 h at 37 °C) before being imaged. **CPD-Ab** (green); Hoechst (blue). Scale bar = 20 μm.

interchain disulfides in the Ab, the TCO reagent underwent double elimination−addition reactions with two cysteines from the same reduced disulfide to form a three-carbon bridge, thus successfully introducing TCO into the Ab while leaving it structurally intake. The same approach has been used for site-specific PEGylation and ADCs in various therapeutic proteins/Abs.[31,32] As shown in Figure 4B, while **Ab^{FC}** showed up on a DTT-free SDS-PAGE gel as a 250-KDa fluorescent band under the FITC channel (lanes 4), successful introduction of the TCO moiety (giving the resulting **TCO-Ab^{FC}**) followed by ligation with a Tz-containing tetraethylrhodamine reporter (TER-Tz2[18]) shifted the band to higher molecular weight regions where they became detectable under both FITC and TER channels (lanes 2).

With **TCO-Ab^{FC}** being successfully prepared, we next conjugated it to $_{Tz}$**CPD**, as earlier described, to generate **CPD-Ab**, which was subsequently used for confirmation of successful intracellular Ab delivery by CLSM. As can be seen in Figure 4C, live HeLa cells treated with 50 nM of **CPD-Ab** for 1 h were shown to have taken up the fluorescently labeled Ab and distributed it throughout the cytosol (right panel), whereas no fluorescence was detected in cells treated with the Ab alone (without conjugation to $_{Tz}$**CPD**; left panel). We thus concluded that this CPD-assisted method could be used for intracellular delivery of Abs as well.

Small-Molecule Drug Delivery by CPD-MSNs. Delivery of small-molecule drugs to tumor sites often suffers from low efficiency due to hydrophobicity and poor water solubility. Approximately 40% of all current commercial drugs and up to 75% of drug candidates are classified as being poorly water-soluble.[3b] We reasoned the siCPD method previously proposed by Matile et al. would have been impractical, as it would require chemical modification of small molecules with a thiol handle which is not available in most native drugs.[12b] We therefore turned to MSNs, which are widely used for intracellular delivery of native small-molecule drugs. Becuase of their large size (>100 nm in diameter), MSNs are often not efficiently taken up by cells unless surface modification with CPPs or other chemicals is introduced.[10,11] In most cases, however, this leads to endocytosis and poor cytosolic release of MSN-encapsulated drugs. We wondered whether the unique endocytosis-independent mechanisms of the CPD-assisted delivery could be successfully emulated in drug-loaded MSNs, e.g., **CPD-MSN-Dox**.

To make **CPD-MSN-Dox**, PO_4^--modified MSNs were first prepared according to published protocols.[33] Such MSNs, due to their negatively charged surface, were known to be minimally taken up by mammalian cells. To follow the cellular uptake of MSNs, they were first doped with a small amount of fluorescein.[11c] We next loaded Dox followed by capping the surface of the resulting drug-loaded MSNs with positively charged $_{Biotin}$**CPD** via charge−charge interaction. The resulting MSNs were shown to be highly monodisperse (mean diameter ca. 155 nm) and possess well-defined pore sizes with high specific areas (Figures S10−S13). Reversal of Zeta potentials from negatives in the PO_4^--modified MSNs to positives in the CPD-capped MSNs was evident (Figure S14). *In vitro* GSH-induced depolymerization/uncapping followed by release of Dox was successfully observed (Figure S15).

To follow the entire process, from cellular uptake of **CPD-MSN-Dox** in live HeLa cells and the subsequent uncapping/depolymerization of CPD to cytosolic release of Dox, we directly added to the cell medium 20 μg/mL of the drug-loaded MSNs, and the resulting cells were imaged over 24 h by CLSM, followed by WB and apoptosis analysis (Figure 5). **MSN-Dox**, the drug-loaded NPs without capping with $_{Biotin}$**CPD**, was used as a negative control. Since Dox is an intrinsically fluorescent compound, its intracellular distribution could be conveniently monitored by CLSM. It is also one of the most effective anti-cancer drugs. By intercalating to nuclear DNA of target tumors, it is known to cause caspase-3 activation, PARP1 cleavage, and cell apoptosis.[34] As shown in Figure 5A, we observed accumulation of most **CPD-MSN-Dox** inside the cytosol of treated cells after only 3 h of incubation, at which point substantial release of the MSN-encapsulated Dox (in red) was also observed (panels 1−3). The slower cellular uptake of **CPD-MSN-Dox**, when compared to that of **CPD-Protein**, was likely due to the much larger size of MSNs, but was nevertheless still faster than that of CPP-capped MSNs.[11] Over the course of the next 21 h, more Dox was released from **CPD-MSN-Dox** and entered cell nucleus (panels 6, 10, and 14 in Figure 5A), resulting in apoptosis in >70% of cells (Figure 5B,C; 24 h treatment). Successful activation of endogenous caspase-3 activity and cleavage of PARP1 were observed as well. For cells treated with **MSN-Dox** (i.e., no $_{Biotin}$**CPD** capping; 12 and 24 h incubation), intracellular fluorescence signals were detected in the red but not green channel, indicating that cellular uptake of **MSN-Dox** was unsuccessful due to a lack of the surface-bound $_{Biotin}$**CPD** (Figure S16), but Dox leaked from the NPs was able to subsequently enter cells freely and cause cell death. Again, a small percentage of cell death detected in cells treated with **CPD-MSN** (i.e., no Dox; Figure 5C) was attributed to the trace amount of iodoacetamide present in $_{Biotin}$**CPD**.

DOI: 10.1021/jacs.5b08130
J. Am. Chem. Soc. 2015, 137, 12153−12160

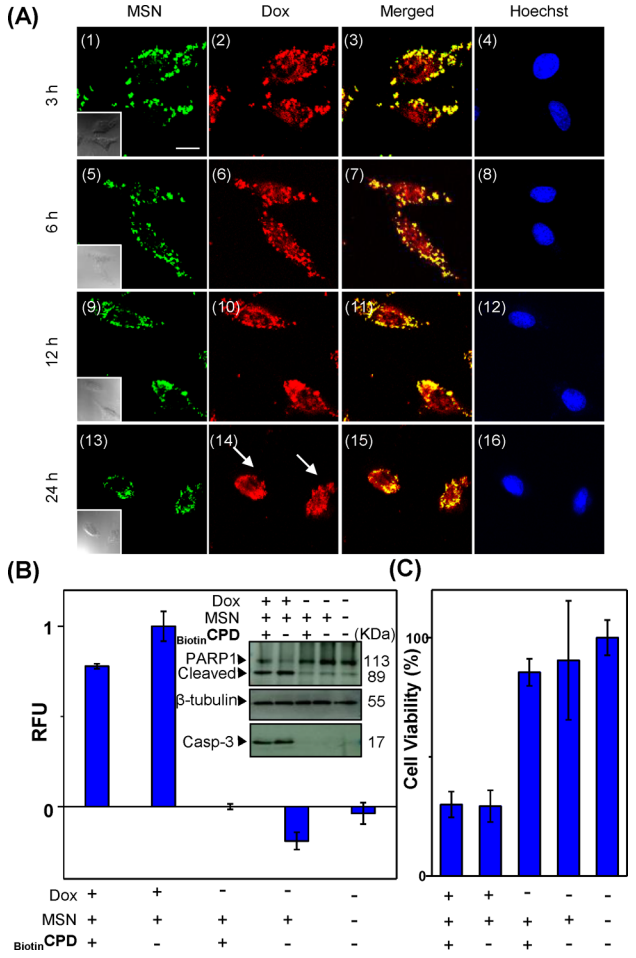

Figure 5. (A) Confocal images of HeLa cells treated with **CPD-MSN-Dox** (20 μg/mL) over 24 h at 37 °C. Dox (red), MSN (green), and Hoechst (blue) were colored accordingly. Arrows indicate apoptotic cells. Scale bar = 20 μm. (B) *In vitro* enzymatic assay of the cell lysates (after 24 h cell treatment). RFU was recorded after 5 h incubation with Ac-DEVD-AMC (1 μM) with HeLa lysate (25 μg/reaction). Inset: WB results showing the successful activation of endogenous caspase-3 and cleavage of PARP1 of treated cells. (C) Cell viability/apoptosis caused by release of intracellular Dox in panels (A) and (B) as measured by XTT assay. Control experiments were concurrently done with cells treated with MSNs alone, **CPD-MSN** or **MSN-Dox**.

CONCLUSION

In this study, we have successfully designed and synthesized several novel cell-penetrating poly(disulfide)s. These CPDs ($_{Biotin}$**CPD**, $_{Ni\text{-}NTA}$**CPD**, and $_{Tz}$**CPD**)—upon highly efficient bioorthogonal "conjugation", either non-covalently or covalently, to readily available cargos, including recombinant proteins and suitably modified antibodies—were able to rapidly and efficiently deliver these cargos into different mammalian cells via endocytosis-independent pathways. Rapid intracellular CPD depolymerization of the delivered cargos under highly reduced cytosolic environments subsequently released the proteins in their functionally active form, which could then be further translocated to their intended subcellular organelles for additional biological processes. The successful intracellular delivery of antibodies by $_{Tz}$**CPD** indicates that this method may be more broadly applicable in the future for effective cellular delivery of many other therapeutic antibodies, which at present could not be adequately achieved with other protein transduction methods.[15] Unlike the siCPDs approach recently developed by Matile et al.,[12b] who suggested that thiol-containing small-molecule drugs and probes may be directly "grown" onto CPDs during polymerization, we have successfully developed CPD-capped MSNs for encapsulation of native small-molecule drugs without the need to introduce thiol handles. With doxorubicin as an example, we found that **CPD-MSN-Dox** entered mammalian cells rapidly and was able to subsequently release free Dox into the cytosol. While more studies are needed to investigate the utility of CPDs as novel "capping" agents for MSNs and other types of nanoparticles, our preliminary findings reported herein indicate that they may be widely used in the future for intracellular delivery of otherwise difficult-to-deliver drugs in a highly controllable manner.[3,10]

Key features of our two-step, CPD-assisted approaches are their versatility and flexibility, enabling immediate delivery of a variety of cargos (recombinant proteins, antibodies, and native small-molecule drugs) with minimal chemical and genetic manipulations. Another feature is the rapid and "bioorthogonal" cargo-loading process: with different types of pre-synthesized CPDs in hand, the resulting CPD−cargo conjugates could be prepared in a matter of minutes under aqueous conditions and used immediately for subsequent cell delivery studies. The minimal cell cytotoxicity of these new CPDs and their cargo-loaded conjugates further highlights the unique advantage of this new cell-transduction method over other existing strategies and ensures that our entire delivery protocol is compatible with live-cell experiments. Future work will focus on expansion of the types of CPDs by using other conjugation chemistries, development of better CPD purification protocols, and application of these CPDs for cell-type-specific delivery of other therapeutically important drugs (including proteins, antibodies, and small molecules).

ASSOCIATED CONTENT

Supporting Information

The Supporting Information is available free of charge on the ACS Publications website at DOI: 10.1021/jacs.5b08130.

Other relevant experimental details, spectral characterizations of compounds, and supplementary biological results (PDF)

Supplementary video S1, complete 3D views of HeLa cells after CPD-BSA treatment for 15 min (ZIP)

Supplementary video S2, complete 3D views of HeLa cells after CPD-BSA treatment for 30 min (ZIP)

Supplementary video S3, complete 3D views of HeLa cells after CPD-BSA treatment for 60 min(ZIP)

Supplementary video S4, complete 3D views of HeLa cells after CPD-BSA treatment for 120 min (ZIP)

Supplementary video S5, complete 3D views of HeLa cells after CPD-BSA treatment for 240 min (ZIP)

AUTHOR INFORMATION

Corresponding Author

*chmyaosq@nus.edu.sg

Notes

The authors declare no competing financial interest.

ACKNOWLEDGMENTS

Funding was provided by the Singapore National Medical Research Council (CBRG/0038/2013) and the Ministry of

DOI: 10.1021/jacs.5b08130
J. Am. Chem. Soc. 2015, 137, 12153−12160

Education (MOE2013-T2-1-048). We also acknowledge Shikun Nie (NUS) for synthesis of CPDs and their monomers.

REFERENCES

(1) Torres, A. G.; Gait, M. J. *Trends Biotechnol.* **2012**, *30*, 185−190.
(2) (a) Fu, A.; Tang, R.; Hardie, J.; Farkas, M. E.; Rotello, V. M. *Bioconjugate Chem.* **2014**, *25*, 1602−1608. (b) van den Berg, A.; Dowdy, S. F. *Curr. Opin. Biotechnol.* **2011**, *22*, 888−893. (c) Lindsay, M. A. *Curr. Opin. Pharmacol.* **2002**, *2*, 587−594. (d) Mintzer, M. A.; Simanek, E. E. *Chem. Rev.* **2009**, *109*, 259−302. (e) Nguyen, J.; Szoka, F. C. *Acc. Chem. Res.* **2012**, *45*, 1153−1162. (f) Kostarelos, K.; Miller, A. D. *Chem. Soc. Rev.* **2005**, *34*, 970−994.
(3) (a) Sun, T.; Zhang, Y. S.; Pang, B.; Hyun, D. C.; Yang, M.; Xia, Y. *Angew. Chem., Int. Ed.* **2014**, *53*, 12320−12364. (b) Williams, H. D.; Trevaskis, N. L.; Charman, S. A.; Shanker, R. M.; Charman, W. N.; Pouton, C. W.; Porter, C. J. *Pharmacol. Rev.* **2013**, *65*, 315−499. (c) Jorgensen, W. L.; Duffy, E. M. *Adv. Drug Delivery Rev.* **2002**, *54*, 355−366.
(4) (a) Heitz, F.; Morris, M. C.; Divita, G. *Br. J. Pharmacol.* **2009**, *157*, 195−206. (b) Montrose, K.; Yang, Y.; Sun, X.; Wiles, S.; Krissansen, G. W. *Sci. Rep.* **2013**, *3*, 1661−1667. (c) Nischan, N.; Herce, H. D.; Natale, F.; Bohlke, N.; Budisa, N.; Cardoso, M. C.; Hackenberger, C. P. R. *Angew. Chem., Int. Ed.* **2015**, *54*, 1950−1953.
(5) (a) Zuris, J. A.; Thompson, D. B.; Shu, Y.; Guilinger, J. P.; Bessen, J. L.; Hu, J. H.; Maeder, M. L.; Joung, J. K.; Chen, Z. Y.; Liu, D. R. *Nat. Biotechnol.* **2015**, *33*, 73−80. (b) Cronican, J. J.; Thompson, D. B.; Beier, K. T.; McNaughton, B. R.; Cepko, C. L.; Liu, D. R. *ACS Chem. Biol.* **2010**, *5*, 747−752.
(6) (a) Allen, T. M.; Cullis, P. R. *Adv. Drug Delivery Rev.* **2013**, *65*, 36−48. (b) Sarker, S. R.; Hokama, R.; Takeoka, S. *Mol. Pharmaceutics* **2014**, *11*, 164−174.
(7) Han, D. H.; Na, H. K.; Choi, W. H.; Lee, J. H.; Kim, Y. K.; Won, C.; Lee, S. H.; Kim, K. P.; Kuret, J.; Min, D. H.; Lee, M. J. *Nat. Commun.* **2014**, *5*, 5633.
(8) (a) Tunnemann, G.; Martin, R. M.; Haupt, S.; Patsch, C.; Edenhofer, F.; Cardoso, M. C. *FASEB J.* **2006**, *20*, 1775−1784. (b) Richard, J. P.; Melikov, K.; Vives, E.; Ramos, C.; Verbeure, B.; Gait, M. J.; Chernomordik, L. V.; Lebleu, B. *J. Biol. Chem.* **2003**, *278*, 585−590.
(9) Michaudel, Q.; Journot, G.; Regueiro-Ren, A.; Goswami, A.; Guo, Z.; Tully, T. P.; Zou, L.; Ramabhadran, R. O.; Houk, K. N.; Baran, P. S. *Angew. Chem., Int. Ed.* **2014**, *53*, 12091−12096.
(10) (a) Nicolas, J.; Mura, S.; Brambilla, D.; Mackiewicz, N.; Couvreur, P. *Chem. Soc. Rev.* **2013**, *42*, 1147−1235. (b) Li, Z.; Barnes, J. C.; Bosoy, A.; Stoddart, J. F.; Zink, J. I. *Chem. Soc. Rev.* **2012**, *41*, 2590−2605. (c) Coll, C.; Bernardos, A.; Martinez-Manez, R.; Sancenon, F. *Acc. Chem. Res.* **2013**, *46*, 339−349.
(11) (a) Zhang, P.; Cheng, F.; Zhou, R.; Cao, J.; Li, J.; Burda, C.; Min, Q.; Zhu, J. *Angew. Chem., Int. Ed.* **2014**, *53*, 2371−2375. (b) Slowing, I. I.; Trewyn, B. G.; Lin, V. S. Y. *J. Am. Chem. Soc.* **2006**, *128*, 14792−14793. (c) Yu, C.; Qian, L.; Uttamchandani, M.; Li, L.; Yao, S. Q. *Angew. Chem., Int. Ed.* **2015**, *54*, 10574−10578.
(12) (a) Bang, E.-K.; Gasparini, G.; Molinard, G.; Roux, A.; Sakai, N.; Matile, S. J. *J. Am. Chem. Soc.* **2013**, *135*, 2088−2091. (b) Gasparini, G.; Bang, E.-K.; Molinard, G.; Tulumello, D. V.; Ward, S.; Kelley, S. O.; Roux, A.; Sakai, N.; Matile, S. *J. Am. Chem. Soc.* **2014**, *136*, 6069−6074. (c) Chuard, N.; Gasparini, G.; Roux, A.; Sakai, N.; Matile, S. *Org. Biomol. Chem.* **2015**, *13*, 64−67. (d) Gasparini, G.; Sargsyan, G.; Bang, E. K.; Sakai, N.; Matile, S. *Angew. Chem., Int. Ed.* **2015**, *54*, 7328−7331.
(13) Son, S.; Namgung, R.; Kim, J.; Singha, K.; Kim, W. J. *Acc. Chem. Res.* **2012**, *45*, 1100−1112.
(14) Gasparini, G.; Bang, E.-K.; Montenegro, J.; Matile, S. *Chem. Commun.* **2015**, *51*, 10389−10402.
(15) Marschall, A. L.; Frenzel, A.; Schirrmann, T.; Schüngel, M.; Dübel, S. *mAbs* **2011**, *3*, 3−16.
(16) (a) Khalili, H.; Godwin, A.; Choi, J. W.; Lever, R.; Brocchini, S. *Bioconjugate Chem.* **2012**, *23*, 2262−2277. (b) Polytherics Home Page. http://www.polytherics.com (accessed Sept 2, 2015). (c) Click Chemistry Tools Home Page. https://www.clickchemistrytools.com (accessed Sept 2, 2015).
(17) Devaraj, N. K.; Weissleder, R. *Acc. Chem. Res.* **2011**, *44*, 816−827.
(18) Li, Z.; Wang, D.; Li, L.; Pan, S.; Na, Z.; Tan, C. Y. J.; Yao, S. Q. *J. Am. Chem. Soc.* **2014**, *136*, 9990−9998.
(19) Zhang, C.; Tan, C. Y. J.; Ge, J.; Na, Z.; Chen, G. Y. J.; Uttamchandani, M.; Sun, H.; Yao, S. Q. *Angew. Chem., Int. Ed.* **2013**, *52*, 14060−14064.
(20) Katz, B. A. *J. Mol. Biol.* **1997**, *274*, 776−800.
(21) (a) Fuchs, S. M.; Raines, R. T. *ACS Chem. Biol.* **2007**, *2*, 167−170. (b) McNaughton, B. R.; Cronican, J. J.; Thompson, D. B.; Liu, D. R. *Proc. Natl. Acad. Sci. U. S. A.* **2009**, *106*, 6111−6116.
(22) (a) ThermoFisher Home Page. http://www.thermofisher.com/order/catalog/product/89850 (accessed Sept 3, 2015). (b) Zelphati, O.; Wang, Y.; Kitada, S.; Reed, J. C.; Felgner, P. L.; Corbeil, J. *J. Biol. Chem.* **2001**, *276*, 35103−35110.
(23) Denault, J. B.; Salvesen, G. S. *Chem. Rev.* **2002**, *102*, 4489−4499.
(24) Yang, X. H.; Sladek, T. L.; Liu, X.; Butler, B. R.; Froelich, C. J.; Thor, A. D. *Cancer Res.* **2001**, *61*, 348−354.
(25) Ng, S. L.; Yang, P.-Y.; Chen, K. Y.-T.; Srinivasan, R.; Yao, S. Q. *Org. Biomol. Chem.* **2008**, *6*, 844−847.
(26) (a) Li, J.; Yao, S. Q. *Org. Lett.* **2009**, *11*, 405−408. (b) Hu, M.; Li, L.; Wu, H.; Su, Y.; Yang, P.-Y.; Uttamchandani, M.; Xu, Q.-H.; Yao, S. Q. *J. Am. Chem. Soc.* **2011**, *133*, 12009−12020.
(27) Na, Z.; Peng, B.; Ng, S.; Pan, S.; Lee, J.-S.; Shen, H. M.; Yao, S. Q. *Angew. Chem., Int. Ed.* **2015**, *54*, 2515−2519.
(28) Chaitanya, G. V.; Alexander, J. S.; Babu, P. P. *Cell Commun. Signaling* **2010**, *8*, 31.
(29) Weiner, L. M.; Surana, R.; Wang, S. *Nat. Rev. Immunol.* **2010**, *10*, 317−327.
(30) Lyon, R. P.; Meyer, D. L.; Setter, J. R.; Senter, P. D. *Methods Enzymol.* **2012**, *502*, 123−138.
(31) Shaunak, S.; Godwin, A.; Choi, J.-W.; Balan, S.; Pedone, E.; Vijayarangam, D.; Heidelberger, S.; Teo, I.; Zloh, M.; Brocchini, S. *Nat. Chem. Biol.* **2006**, *2*, 312−313.
(32) Badescu, G.; Bryant, P.; Bird, M.; Henseleit, K.; Swierkosz, J.; Parekh, V.; Tommasi, R.; Pawlisz, E.; Jurlewicz, K.; Farys, M.; Camper, N.; Sheng, X. B.; Fisher, M.; Grygorash, R.; Kyle, A.; Abhilash, A.; Frigerio, M.; Edwards, J.; Godwin, A. *Bioconjugate Chem.* **2014**, *25*, 1124−1136.
(33) Zhao, Y. L.; Li, Z.; Kabehie, S.; Botros, Y. Y.; Stoddart, J. F.; Zink, J. I. *J. Am. Chem. Soc.* **2010**, *132*, 13016−13025.
(34) Tacar, O.; Sriamornsak, P.; Dass, C. R. *J. Pharm. Pharmacol.* **2013**, *65*, 157−170.
(35) Norton, J. T.; Titus, S. A.; Dexter, D.; Austin, C. P.; Zheng, W.; Huang, S. *J. Biomol. Screening* **2009**, *14*, 1045−1053.

DOI: 10.1021/jacs.5b08130
J. Am. Chem. Soc. 2015, 137, 12153−12160